Industrial Crops & Products 113 (2018) 368–375

Contents lists available at ScienceDirect

Industrial Crops & Products

journal homepage: www.elsevier.com/locate/indcrop

Elucidation of structure-inhibition relationship of monosaccharides derived pseudo-lignin in enzymatic hydrolysis

Juan He, Caoxing Huang, Chenhuan Lai, Chen Huang, Xin Li, Qiang Yong*

Co-Innovation Center for Efficient Processing and Utilization of Forest Resources, Nanjing Forestry University, Nanjing, 210037, China

ARTICLE INFO

Keywords:
Acid-pretreatment
Monosaccharide
Lignin
Pseudo-lignin
Cellulase adsorption

ABSTRACT

Pseudo-lignin is defined as aromatic material, which could be formed through dehydration synthesis and aromatisation of carbohydrate. In this work, dilute sulfuric acid was carried out to treat monosaccharides and holocellulose to generate pseudo-lignin and the residual lignin (RL) in acid-pretreated bamboo was isolated. The structural informations of pseudo-lignin were assayed by nondestructive techniques (SEM, FTIR, and ^{31}P NMR). Meanwhile, the nonproductive adsorption performance of pseudo-lignin and cellulase was evaluated, taking RL as the comparison. Results showed that pseudo-lignin represented sensible droplets and was consist of aliphatics, carbonyl and aromatic structures. The amounts of aliphatic hydroxyl groups and carboxylic acid in pseudo-lignin were 0.61–0.79 mmol/g and 0.64–0.68 mmol/g, respectively. Total OH content of RL (3.51 mmol/g) was higher than pseudo-lignins (2.52–3.05 mmol/g). Due to the lower negative surface charge, hydrophobic nature, Langmuir constant (K) and binding strength (R) of pseudo-lignin, it represented weaker negative impact on enzymes than RL.

1. Introduction

Lignocellulosic biomass is an essential resource for sustainably producing energy and chemical products due to its renewable and terrestrial abundance. Methods for biomass conversion into valuable products could be enzymatic (Galbe and Zacchi, 2002; Huber et al., 2006), catalytic (Galbe and Zacchi, 2002; Girisuta et al., 2007) or thermochemical (Sasaki et al., 1998; Bulushev and Ross, 2011). Enzymatic conversion, industrially viewed as moderate with respect to processing severity and societally perceived as “green”, is a biological method for depolymerization cellulose to glucose monomers (Lai et al., 2014). Due to biomass’s natural recalcitrance towards cellulolytic depolymerization, the yield of glucose cellulolytically produced from native lignocellulosic materials is quite low (Narron et al., 2016). As a result, efficient production of fermentable sugars from lignocellulosic biomass requires an efficient pretreatment to overcome recalcitrance barriers.

Pretreatment technologies can degrade the structure of plant cell walls, enabling a greater amount of cellulase accessibility to cellulose and high yield of monosaccharide production would be achieved. Dilute acid pretreatment has universality for various biomass, so it is widely applied in pretreating of biomass’ conversion. It consists of acidic solution, heat, pressure and retention time ranging from less than 1 min to 60 min. In general, the concentration of H_2SO_4 carried out with 0.4–2.0 wt% at a temperature of 140–200 °C (Pu et al., 2013). During acid pretreatment, most hemicellulose could be degraded into various oligosaccharides and monosaccharide in some degree. Besides, few amount of lignin could be removed and the ether connections between cinnamic acid and lignin would be break down effectively, which could improve cellulose accessibility of biomass (Narron et al., 2016). Synthetically, it is a kind of potential cost-effective methods that can improve the release performance of monosaccharides with lower processing cost (Hu and Ragauskas, 2012; Jung et al., 2010). However, with higher combined severity factor, pretreated biomass did not emerge more significant delignification. Undesired inter-lignin condensation reactions would play major role in acidolysis and cause the inhibition of saccharification (Ko et al., 2015). On the other hand, dilute acid-pretreated biomass show higher content of acid-insoluble lignin (Klason lignin) than the primary material (Chen et al., 2010; Pingali et al., 2010), which has been hypothesized to the formation of pseudo-lignin (Sannigrahi et al., 2011; Li et al., 2007). Sannigrahi et al. (2011) has confirmed that carbohydrates alone could be responsible for the formation of pseudo-lignin through dehydration with acid catalysis during pretreatment process.

During dilute acid pretreatment, acetic acid is cleaved from hemicellulose which can decrease the pH value of the cooking liquor further (Mosier et al., 2005). Lower pH reaction liquid and higher pretreatment temperatures promote monosaccharide to generate few reaction

* Corresponding author.
E-mail address: swhx@njfu.com.cn (Q. Yong).

https://doi.org/10.1016/j.indcrop.2018.01.046
Received 25 September 2017; Received in revised form 13 January 2018; Accepted 19 January 2018

pathways, which proceed furfural, 5-hydroxymethylfurfural (HMF), and ended up with levulinic acid (LA) (Baugh and McCarty, 1988; Chang et al., 2009). Besides, LA is considered to be the parallel formation of dark colored solids, which are defined as pseudo-lignin. The amount of LA has a negative correlation with pseudo-lignin formation (Patil and Lund, 2011). Acid-catalysis of HMF has been reported to involve two reaction pathways, one involving formation of LA and the other involves production of pseudo-lignin (Horvat et al., 1985; Horvat et al., 1986). However, the specific mechanism for pseudo-lignin generation remains unclear.

Researchers reported that the elemental composition of pseudo-lignin was determined as 55–65% carbon, 4–5% hydrogen and 30–40% oxygen (Girisuta et al., 2006). Scanning electron microscope (SEM) of pseudo-lignin displayed that pseudo-lignin exists as the same agglomerated spherical particles akin to dissolved lignin droplets (Girisuta et al., 2007). ^{13}CP/MAS NMR analysis of pretreated holocellulose proved that pseudo-lignin has some carbonyl, aromatic, metheoxy and aliphatic structures. Furthermore, increasing pretreatment severity lead to an increase in the presence of the aforementioned structures (Sannigrahi et al., 2011).

It has been hypothesized that pseudo-lignin could bond with melted lignin and deposit on the surface of lignocellulose, which would block cellulase access to the substrate and decrease enzymatic efficiency (Donohoe et al., 2008; Yang and Wyman, 2006;). Hu et al. (2012) reported that pseudo-lignin could induce a decrease in the enzymatic conversion of Avicel cellulose. For example, with the increased addition of pseudo-lignin from 0.0% to 65.0% (w/w), the cellulose conversion would decrease from 60.0% to 38.0%. In addition, it has also been reported that pseudo-lignin could non-productively bind to enzyme and reduce the efficiency of enzymatic hydrolysis (Zhuang et al., 2016). Therefore, from the biofuel production perspective, it's significant to further understand the inhibitory mechanisms empirically observed between cellulolytic enzymes and pseudo-lignin.

Although the generation of pseudo-lignin from avicel cellulose or holocellulose has been reported by many researchers (Hu et al., 2012; Jakobsons et al., 1995), there has been a lack of fundamental characterization of the pseudo-lignins formed from monosaccharides like glucose and xylose. Hence, in this work, appearance of pseudo-lignin (formed from monosaccharide), holocellulose and pretreated holocellulose were revealed by SEM. In addition, Residual lignin (RL) was taken as a reference, ^{31}P NMR was performed upon the pseudo-lignin in order to understand if there is any structural similarity between them. Then, the surface charge, hydrophobic nature and Langmuir adsorption isotherm parameters of pseudo-lignin and RL were also measured to understand the different impacts of pseudo-lignins and RL on enzymatic efficiency and cellulase adsorption.

2. Materials and methods

2.1. Materials

Bamboo residues (*Phyllostachys heterocycla*) were obtained from the He Qi Cang Bamboo Processing Factory (Fujian, China). The air-dried samples were milled to 20–80 mesh particle size. The chemical components of bamboo residues were as follows (%, dry weight basis): 39.5% glucan, 20.8% xylan, 30.7% total lignin. Holocellulose was isolated from the extractive-free bamboo residues using sodium chlorite bleaching (Hubbell and Ragauskas, 2010). Monosaccharide standards (including glucose and xylose) were purchased from Ronghua chemicals in Nanjing, China. Cellulase cocktail (L-100, with an activity of 188.54 FPU/g) was kindly provided by Youtell Biochemical Co., Ltd (China) (Fig. 1).

2.2. Dilute sulfuric acid pretreatment

Bamboo residues, monosaccharides (pure glucose, pure xylose, mixture of glucose and xylose with ratio of 1:1 and 1.9:1) and holocellulose were pretreated by dilute sulfuric acid in 1-L autoclave bombs that were heated with an oil bath. The sulfuric acid charge was 2% (w/v) and the ratio of dried solid to liquid was 1:10. Pretreatment lasted for 60 min at 180 °C. After pretreatment, the solids were separated from slurry and washed with distilled water until resultant filtrate was neutral.

Bamboo residues used for enzymatic hydrolysis was treated at 120 °C with 0.5% sulfuric acid charge, other conditions was the same as above.

2.3. Extraction of pseudo-lignin

Solid formed from monosaccharides and acid-pretreated holocellulose were regarded as pseudo-lignin. They were extracted by solvent (dioxane/water (24:1, v/v) with a ratio of solid-to-solvent 1:20 (g: ml). After extraction, the mixtures were centrifuged at 8000 rpm for 5 min and the supernatant separated through a filter funnel. This procedure was repeated three times with addition of new solvent at each stage. The mixed filtrates were evaporated under vacuum to remove dioxane solution. Finally, extracted pseudo-lignins were vacuum-dried at 40 °C to constant weight.

2.4. Isolation and purification of residual lignin in pretreated bamboo residues

The residual lignin (RL) in dilute-acid pretreated bamboo residues (carried out as described in Section 2.2) was extracted according to the method established by Björkman (1954). Specific experimental procedures were according to our previous work (Huang et al., 2016a).

2.5. Enzymatic hydrolysis of pretreated bamboo residues with pseudo-lignin and RL

Enzymatic hydrolysis of pretreated bamboo residues was carried out in 50 mL of 0.05 M sodium citrate buffer (pH 4.8) at 5% substrate (w/v) with cellulase and β-glucosidase loadings of 30 FPIU/g and 10 IU/g, respectively. The amounts of pseudo-lignins and RL suspended in the saccharification medium were 5% (w/w). Enzymatic hydrolysis was performed at 50 °C with 150 rpm agitation for 48 h. Enzymatic hydrolysis efficiency of pretreated samples was calculated as following equation:

$$Y = \frac{glucose\ in\ enzymatic\ hydrolysate(g)}{inital\ glucose\ in\ substrate(g)} \times 100\%$$

2.6. Cellulase adsorption on pseudo-lignin and RL

Adsorption experiments for pseudo-lignins (generated from pure glucose and xylose) and RL were carried out for 0.5, 1, 3, 6, 9, 24, 48 h at 50 °C in a rotary shaker at 150 rpm. The experiments were carried out in 0.05 M citrate buffer (pH 4.8) system with 0.25% (w/v) dried samples. The supernatants were used to analyze cellulase activity and protein content. Cellulase activity was determined according to the IUPAC standard protocol (Ghose, 1987). The protein content was measured based on Bradford method, with bovine serum albumin used as protein standard (Bradford, 1976).

2.7. Cellulase adsorption isotherm on pseudo-lignin and RL

Cellulase adsorption upon pseudo-lignins and RL was performed at 50 °C. A range of enzyme concentrations from 0.01 to 1.0 mg/mL were added in 0.5 M citrate buffer (pH 4.8) with the samples at 0.5% (w/v) and incubated at 150 rpm for 3 h to reach equilibrium (Huang et al., 2016b; Lai et al., 2014). After incubation, the mixture was centrifuged

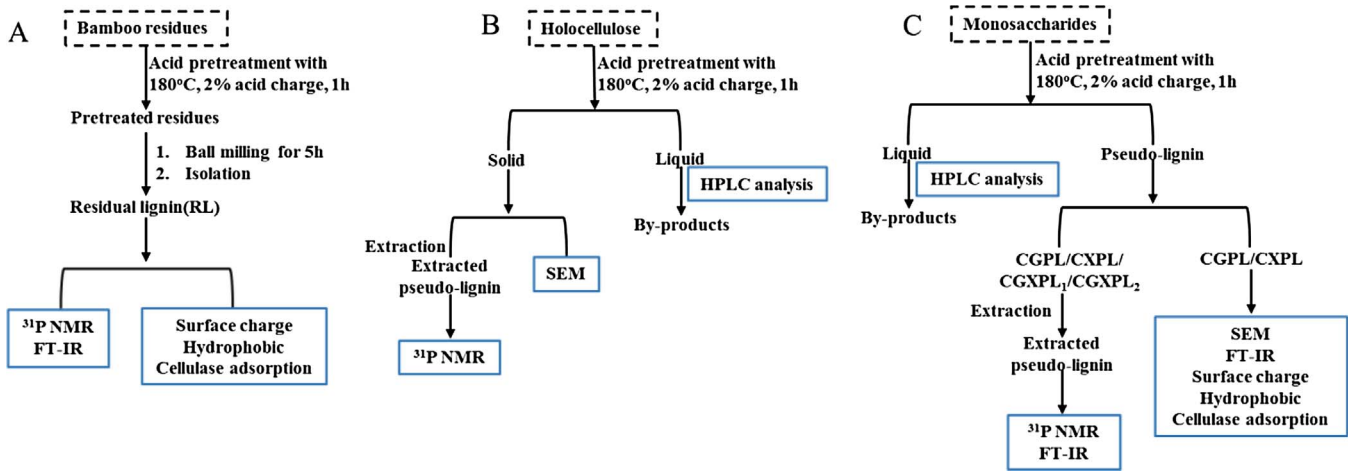

Fig. 1. Scheme of analysis methods for pseudo-lignins and residual lignin (A: residual lignin; B: pseudo-lignin collected from pretreated holocellulose; C: pseudo-lignins collected from pretreated monosaccharides).

at 4000 rpm for 5 min and the free cellulase in supernatant was determined by Bradford assay. The adsorbed cellulase was calculated from the difference between initial enzyme protein content and the free enzyme protein content in supernatant.

The Langmuir adsorption isotherm was applied to characterize cellulose adsorption on pseudo-lignin and RL. In this case, the surface concentration of adsorbed enzymes (Γ) was given by the equation as follows:

$$\Gamma = \frac{\Gamma maxKC}{1 + KC} R = \Gamma maxK$$

Where Γ is the corresponding adsorbed cellulase on the sample (mg/g sample), Γ_{max} is the maximum adsorption capacity (mg/g sample), K is the Langmuir constant (ml/mg), C is the free cellulase in supernatant (mg/ml), and R is the distribution coefficient (L/g).

2.8. Composition analysis of substrates

The carbohydrate and lignin content of pseudo-lignins, holocellulosse and pretreated holocellulose were determined according to the National Renewable Energy Laboratory (NREL) analysis method for samples (Sluiter et al., 2008). Sugar content in the supernatants was quantified by a high performance liquid chromatography system (HPLC). The HPLC system was equipped with an Aminex HPX-87H column (300 × 7.8 mm) and a refractive index (RI) detector. 5 mM H_2SO_4 solution was used as the mobile phase, flowing at a rate of 0.6 mL/min. Reported carbohydrate and lignin composition in the present study were performed in duplicate.

2.9. Analysis of pseudo-lignin and RL

2.9.1. Scanning electron microscopy (SEM)

Imaging of pseudo-lignins, pretreated holocellulose and untreated holocellulose were acquired using a FEI Quanta 400 (HITACHI, Japan), operated at 15 kV. All samples subjected SEM were freeze-dried and coated with gold/palladium (Au/Pd) by a SC7640 automatic/manual high-resolution sputter coater (Quorum Technologies, Newhaven, U.K.). Performance of metal spraying was did on the surface of samples for 100 s to protect samples avoiding been degraded.

2.9.2. FTIR-ATR spectroscopic analysis

Pseudo-lignins and extracted pseudo-lignin were characterized by the Spectrum One FT-IR system (Themor, USA, Thermo nicolet 360) with a universal attenuated total reflection (ATR) accessory was taken to characterize various samples. All samples were dried at 60 °C and flaked with KBr. The wavelength region was 4000–400 cm^{-1} at 2 cm^{-1} resolution.

2.9.3. ^{31}P NMR spectroscopic analysis

Quantitative ^{31}P NMR spectra of extracted pseudo-lignins and RL were acquired by a Bruker AVANCE 600 MHz spectrometer as follows: first, an accurate weight (about 40 mg) of dried samples was added into a NMR tube with 500 μL mixture of anhydrous pyridine and $CDCl_3$ (1.6:1, v/v). Once the samples dissolved, 200 μL of *endo*-N-hydroxy-5-norbornene-2, 3-dicarboximide (e-NHI) solution (9.23 mg/mL acting as internal standard) and 50 μL of chromium (III) acetylacetonate solution (5.6 mg/mL acting as relaxation reagent) were added. Finally, 100 μL of 2-chloro-4, 4, 5, 5-tetramethyl-1, 2, 3-dioxaphospholane (serving as phosphitylating reagent) was added to the NMR tube and inverted for mixing. The prepared sample was finally subjected to immediate ^{31}P NMR analysis (Cui et al., 2014).

2.9.4. Surface charge analysis

The surface charge of RL and pseudo-lignins were determined according to potentiometric titration method (Huang et al., 2016b; Lai et al., 2014). The samples to be measured were firstly dissolved in 10.0 g NaOH solution (0.1 M) and acidified by 3.0 g HCl (1 M) for 10 min by stirring. After that, 30 g NaOH solution (0.1 M) was added to the solution to neutralize the acid and redissolve the dried samples. The sample solution was titrated by 0.1 M HCl solution with the automatic titrator (AUT-701, DKK-TOA) from 12.0 to 2.0. Blank solution (without dried sample) was also processed and titrated. The surface charge (mmol/g) on the samples was calculated as follows: $Q = (V_{blank} - V_{sample}) \times M/W$, where Q is the surface charge of sample, V_{blank} and V_{sample} are the titration volume consumed by sample solution and blank solution, respectively, M is the mole concentration of HCl, and W is the weight of lignin sample.

2.9.5. Hydrophobicity estimation by rose Bengal adsorption

The hydrophobicity of pseudo-lignins and RL was estimated by measuring the distribution of Rose Bengal (hydrophobic dye) in the solution and on the dried samples (Huang et al., 2016b; Lai et al., 2014). In brief, a constant concentration of Rose Bengal (40 mg/L, melted in 0.05 M citrated buffer) was suspended with a range of dried samples concentrations 2–10 g/L. To distribute the hydrophobic dye between dried samples and the solution, the suspension was incubated at 50 °C, 150 rpm for 2 h. After time, the adsorbed dye and samples were separated by centrifugation. The free adsorbed dye was dispersed in the supernatant, and the content was determined by detecting the absorption at 543 nm using a UV–vis spectrometer. The adsorbed dye

Table 1
Lignin and carbohydrate contents of pseudo-lignin, holocellulose and acid-pretreated holocellulose.

Sample[a]	Lignin (%)	Xylan (%)	Glucan (%)	Pseudo-lignin yield[b] (%)	Extracted pseudo-lignin yield[c] (%)
CGPL	90.2 ± 1.3	–	–	25.1	3.1
CXPL	84.1 ± 2.6	–	–	25.1	2.7
$CGXPL_{1(1:1)}$	86.0 ± 1.0	–	–	24.8	2.3
$CGXPL_{2(1.9:1)}$	89.3 ± 2.6	–	–	23.4	2.7
Pretreated-holocellulose	20.4 ± 1.6	1.2 ± 0.2	71.4 ± 1.0	45.1	5.4
Holocellulose	8.0 ± 0.1	27.3 ± 0.2	51.5 ± 0.1	–	–

[a] Pseudo-lignin, which was gained from sulfuric acid pretreated glucose, xylose and various ratio of glucose and xylose (1:1 and 1.9:1, w/w).
[b] Calculated as following: recovered dried solids/initial dried solids*100%.
[c] Calculated as following: extracted dried solids/recovered dried solids *100%.

quantity was calculated by the difference between the initial dye content and the free adsorbed dye content in solution. The partition quotient (PQ) was calculated from the ratio of the adsorbed dye to free dye. The obtained PQ was plotted against sample loading. The surface hydrophobicity of various samples was determined by the slope of the linear plotting (mL/g).

3. Results and discussion

3.1. The formation of pseudo-lignins and its quantitative yields

In order to demonstrate pure monomeric carbohydrate can be converted into pseudo-lignin, dilute sulfuric acid digestion was applied to monomeric carbohydrate solution and the resulted solids were collected. The pseudo-lignins generated from pure glucose, pure xylose, mixture of glucose and xylose with ratio of 1:1 and 1.9:1 were termed as CGPL, CXPL, $CGXPL_1$ and $CGXPL_2$, respectively. The compositions of pseudo-lignin, holocellulose and pretreated holocellulose are displayed in Table 1. After pretreatment, the measured lignin content of holocellulose was greater than what was measured in the original holocellulose, increasing from 8.0% to 20.4%. It indicated that new lignin was generated from holocellulose after it was pretreated by acid solution. In addition, results from chemical analysis also revealed the absence of residual glucan or xylan in the various pseudo-lignins. It is hypothesized that monosaccharides could be completely degraded and further reacted to generate pseudo-lignins. Table 1 also showed that both xylose and glucose could form the same amount of pseudo-lignin. For example, the pseudo-lignin yields of CXPL and CGPL were both 25.1%. The yield of pseudo-lignin in acid-pretreated holocellulose was 45.1%, which was higher than that of $CGXPL_2$ (23.4%). An explanation for the observed difference in pseudo-lignin yields could be that the minor lignin constituents already present in holocellulose would incorporate with pseudo-lignin during acid-pretreatment.

The appearance of untreated holocellulose and pretreated holocellulose were characterized using SEM technology and the images were shown in Fig. 2. Compared to the untreated holocellulose, a visual plethora of spherical droplets can be observed upon the surface of pretreated-holocellulose. Multiple size dimensions of droplets are observable, ranging from 1 μm to 5 μm in diameter. Fig. 2(c-d) also visualizes the similar droplets from acid digestion of various monosaccharides solution. These observation are in agreement with another researcher's suggestion that the diameter of lignin droplets could range from 5 nm to 10 μm during pretreatment (Donohoe et al., 2008). The SEM images indicate that during acid-pretreatment carbohydrates alone can form spherical droplets with morphology to precipitated lignin droplets, which also has been reported in the works of Donohoe et al. (2008) and Pu et al. (2013).

Fig. 3 presents the quantities of the main by-products in pretreatment hydrolysate, such as formic acid (FA), acetic acid (HAc), Levulinic acid (LA), 5-hydroxymethylfurfural (HMF) and furfural (Baugh and McCarty, 1988; Chang et al., 2009). There is no 5-hydroxymethylfurfural existing in the hydrolysate of CXPL, which is different from CGPL, $CGPL_1$, $CGPL_2$ and CHPL. For this phenomenal, the reason may be that the intermediate of pentoses degradation was furfural, while there was HMF degraded from hexoses (Qian et al., 2005). For HMF and furfural, they are proposed as the original materials for the formation of 1, 2, 4-benzenetriol and 3, 8-dihydroxy-2-methylchromone respectively, which were suggested as the key intermediates of pseudo-lignin's generation (Rasmussen et al., 2014). Fig. 3 and Table 1 showed that the yield of pseudo-lignin increased from 23.4% from 45.1%, while the concentration of LA was decreased from 10.56 g/L to 0.77 g/L. The result is in disagreement with the report of Patil and Lund (2011), which LA is proposed to be parallel formation of pseudo-lignin. One explanation for this may be that the actual degradation for holocellulose is more complicated than monosaccharides. For the preparation of pseudo-lignin generated from holocellulose (CHPL), there were more content of HAc in prehydrosate. The reason is that during acid hydrolysis, organic acids like HAc would be released from hemicellulose (Pielhop et al., 2015).

3.2. Structural characterization of pseudo-lignins and RL

As discussed above, pseudo-lignin could form spherical droplets such as lignin. In order to better understand the chemical substructures present in pseudo-lignin, pseudo-lignin was extracted by dioxane to produce a soluble lignin isolate that is representative of the starting pseudo-lignin. After extraction, there were some residues left. The residues also represented spherical morphology, but it showed smaller agglomerate than CGPL (Fig. 2e). It indicated that mostly pseudo-lignin would dissolve in dioxane and during acid-pretreatment carbohydrate would generate some components without aromatic rings. It is in agreement with the hypothesis that during "polymerization" step, aromatic compounds and oligosaccharides (formed from monosaccharide) would form cross-linked structures (Sun and Li, 2004).

Based on Fig. 4, pseudo-lignin generated from acid-treated glucose (CGPL), xylose (CXPL) and extracted pseudo-lignin generated from acid-treated glucose (GPL) consisted of aliphatics, carbonyl and aromatic structures, each showing different intensities at respective absorption bands. The bands at 2921 cm^{-1} and 1361 cm^{-1} were attributed to C—H stretching and C—H rocking in alphatics, respectively. The peak at 2852 cm^{-1}, 1600 cm^{-1}, 1511 cm^{-1} and 798 cm^{-1} correspond to methoxyl group, C=C stretch and C—H out-of- plane bending in aromatic rings (Hu et al., 2012), respectively. In addition, it was observed that CGPL and CXPL have great similarity between their FT-IR spectra, indicating that pseudo-lignin collected after acid-pretreated glucose or xylose is a similar substance. GPL also has similarity with CGPL and CXPL in their FT-IR spectra. However, GPL has stronger peak intensity at 2921 cm^{-1} and 1511 cm^{-1}, arising from the C—H stretch of alphatics and C=C stretch of aromatic rings, respectively. Based on results got from FT-IR spectra, it is speculated that the extraction of pseudo-lignins did no major structural changes for their structures and the extraction would enhance the peak intensity of aromatic rings.

In this work, the hydroxyl groups in extracted pseudo-lignin generated from acid-treated glucose (GPL), xylose (XPL), varying monosaccharide solution ($GXPL_1$, $GXPL_2$), and holocellulose (HPL) were quantitated by a quantitative ^{31}P NMR methodology (Cui et al., 2014).The results are shown in Table 2. Quantitative ^{31}P NMR results confirmed that pseudo-lignin formed from different monosaccharide have varying hydroxyl contents. The contents of total hydroxyl groups were found to be 2.56 mmol/g and 3.05 mmol/g for HPL and GPL, respectively, higher than what was measured in XPL (1.70 mmol/g). These findings suggest that a greater quantity of dehydration reactions

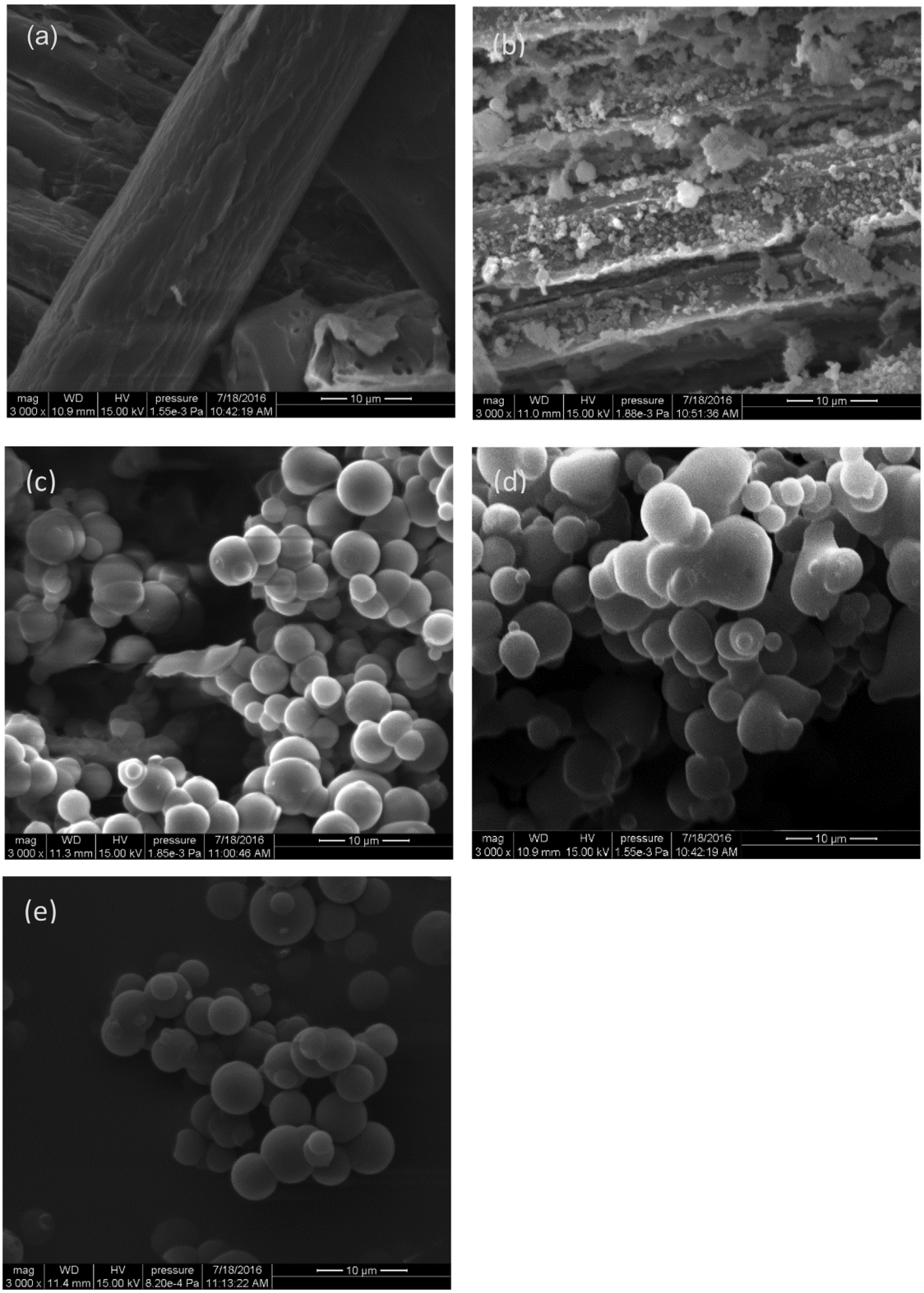

Fig. 2. SEM images of (a) untreated holocellulose, (b) dilute sulfuric acid-pretreated holocellulose, (c) pseudo-lignin collected after acid-pretreated glucose (CGPL), (d) pseudo-lignin collected after acid-pretreated xylose (CXPL), (e) residues collected after dioxane extracted CGPL(GPL).

during the formation of CXPL (Wen et al., 2013). Table 2 also indicated that different ratio of glucose and xylose as a starting monosaccharide solution exerted little impact on the hydroxyl functional group contents of each respective pseudo-lignin. Compare to RL (1.37 mmol/g), the lower amount of aliphatic hydroxyl groups in pseudo-lignin (0.61-0.79 mmol/g) might be attributed to the dehydration reaction and aromatization during acid-pretreatment or it could be that pseudo-lignins does not feature side chain structure (Hu, 2014). Pseudo-lignins were also observed to bear greater amounts of carboxylic acid (0.64-0.68 mmol/g) compared to RL (0.22 mmol/g). An explanation for this could be hydroxyl oxidation occurrence during the formation of pseudo-lignin (Sun et al., 2016).

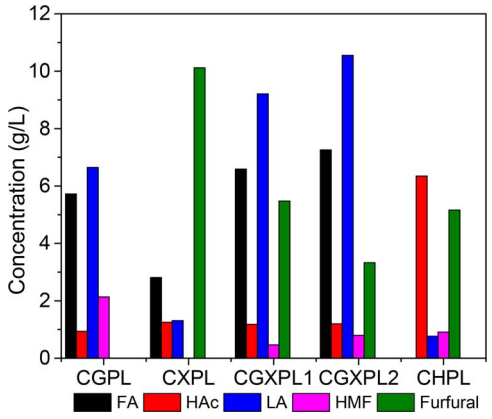

Fig. 3. Concentration of main by-products in pretreatment solution.

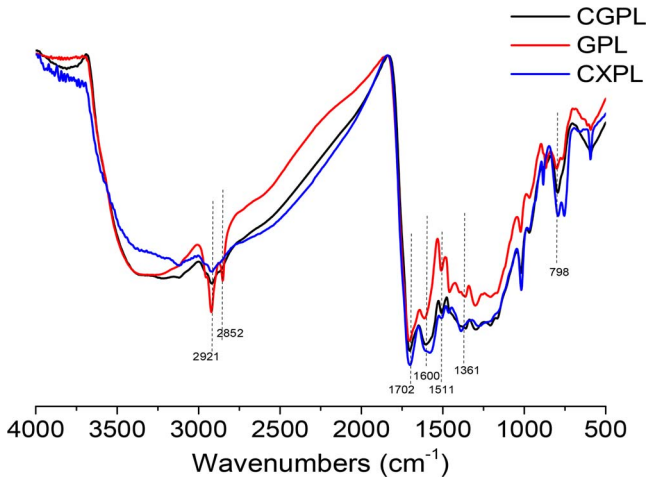

Fig. 4. FT-IR spectra of pseudo-lignin (CGPL, CXPL) and pseudo-lignin (GPL); GPL was extracted from CGPL.

Table 2
Functional group contents obtained by quantitative ^{31}P NMR analyses for RL and various pseudo-lignin.

Sample	OH content (mmol/g)[a]				
	Aliphatic OH	Condensed phenolic OH	Noncondensed phenolic OH	Total OH	COOH
RL	1.37	1.91	1.60	3.51	0.22
HPL	0.79	1.36	1.20	2.56	0.64
GPL	0.62	1.30	1.74	3.05	0.66
XPL	0.70	0.85	0.85	1.70	0.68
$GXPL_1$	0.63	1.20	1.31	2.52	0.66
$GXPL_2$	0.61	1.20	1.38	2.57	0.66

[a] Obtained by quantitative ^{31}P NMR

3.3. Interaction between enzymes and pseudo-lignins and RL

Armed with spectroscopic characterization of pseudo-lignins, we next sought to understand the inhibitory impact of pseudo-lignin (RL for comparison) upon enzymatic hydrolysis of pretreated bamboo residues. The content of pseudo-lignins and residual lignin (RL) in substrate were 5% (w/w). The data showed that enzymatic efficiency of pretreated bamboo residues decreased 0.90%, 0.75%, 0.75%, and 0.70% with the addition of CGPL, CXPL, $CGPL_1$ and $CGPL_2$, respectively. With the addition of RL, the enzyme efficiency was decreased 0.77% (figure is not shown in this article). In order to understand if the pseudo-lignins can inhibitively adsorb cellulase during enzymatic hydrolysis, pseudo-lignins (CGPL and CXPL) and RL were used as substrates for cellulase adsorption experiments (Fig. 5).

As showed in Fig. 5a, the addition of CGPL, CXPL and RL could reduce the activities of cellulase. For example, the addition of CGPL and RL reduced the activities of cellulase from 0.96 FPIU/mL to 0.81 FPIU/mL and 0.77 FPIU/mL, respectively. The addition of CXPL showed similar tendency. Compared with RL, CGPL and CXPL exerted less impact on cellulase activities. Fig. 5b displays that the addition of RL, CGPL, and CXPL also decreases the abundance of free (unadsorbed) cellulase in solution. For example, with the addition of CXPL and RL, the content of free enzyme protein in solution reduced from 0.64 mg/mL to 0.62 mg/mL and 0.55 mg/mL, respectively. The addition of CGPL showed similar tendency. One reason for these observations maybe that lignin and pseudo-lignin's hydrophobic structures enable unproductive binding with cellulase, which contains a number of hydrophobic residues (Huang et al., 2016b). Fig. 5 revealed that RL exerted more inhibitory effects upon enzymes. This could be due to lignin's more hydrophobic nature and content of aliphatic hydroxyl group than pseudo-lignin (Table 2 and Table 3), which showed higher performance in enzyme adsorption (Huang et al., 2016b; Hu et al., 2012). It was found that there was a few differences between the existing results of multi-batch experiments for references in Fig. 5. From One-way ANOVA analysis, it was found that $P_{Blank\text{-}CE} = 0.05$, $P_{Blank\text{-}FE} = 0.00$, $P_{RL\text{-}CE} = 0.03$, $P_{RL\text{-}FE} = 0.00$ (CE: cellulase activity, FA: free enzyme in solution), all of P value is lower than 5%. The statistical analysis results indicated that data of multi-batch experiments was reliable.

Table 3 presents the surface charge and hydrophobicities of pseudo-lignin and RL. The negative surface charges of pseudo-lignin were −2.67 mmol/g and −4.25 mmol/g for CGPL and CXPL, respectively. Both values measured from pseudo-lignins were lower than what was measured in RL (−7.00 mmol/g). Lai et al. (2014) reported that higher negative charges on lignin samples could enhance the electrostatic repulsion and reduce non-productive cellulase binding to lignin. This could play a positive role in terms of enzymatic hydrolysis saccharification yields (Lai et al., 2014). Table 3 also showed that the hydrophobic nature of RL (1665.80 mL/g) is much higher than that of all the pseudo-lignins (59.60–77.45 mL/g), indicated that pseudo-lignin may display a weaker hydrophobic interaction with cellulolytic enzymes. And Fig. 5b represented that there were more free enzymes in the solution with the addition of pseudo-lignin. These results conjectured that during the hydrophobic nature of biological surfaces have more significant effects upon non-productive binding of enzymes.

To further explain the difference of lignin and pseudo-lignin samples on enzyme adsorption, Table 4 summarizes Langmuir adsorption isotherm parameters from enzyme adsorption on samples. The maximum adsorption capacity (Γ_{max}), affinity (K), and binding strength (R) were used to evaluate the interaction between enzymes and substrates (Lai et al., 2014; Hong et al., 2007). CGPL and CXPL showed less affinity with enzymes (K = 3.50 mL/mg and 1.31 mL/mg, respectively), compared to that of RL (K = 13.62 mL/mg). Moreover, the binding strength of RL (R = 2.97 L/g) represented higher than CGPL and CXPL (R = 0.82 and 0.36 L/g, respectively). These maybe the main contributor to the distinct effects of pseudo-lignin and lignin on enzymatic adsorption. It is reported that higher R and K values correlate with lignin's non-productive cellulase binding tendencies (Lai et al., 2014). The main conclusion from the conducted adsorption experiments is that enzymatic efficiency of acid pretreated biomass can be inhibited by carbohydrate-derived pseudo-lignin. To curb this effect, the intensity of dilute acid-pretreatment should be in suitable range for avoiding the formation of pseudo-lignin.

4. Conclusions

Finding indicated that during dilute acid-pretreatment, soluble carbohydrate do further react form insoluble pseudo-lignin. Pseudo-lignin, with the morphology of insoluble droplets suspended in aqueous medium, is comprised of carbonyl, carboxylic, aliphatic and aromatic

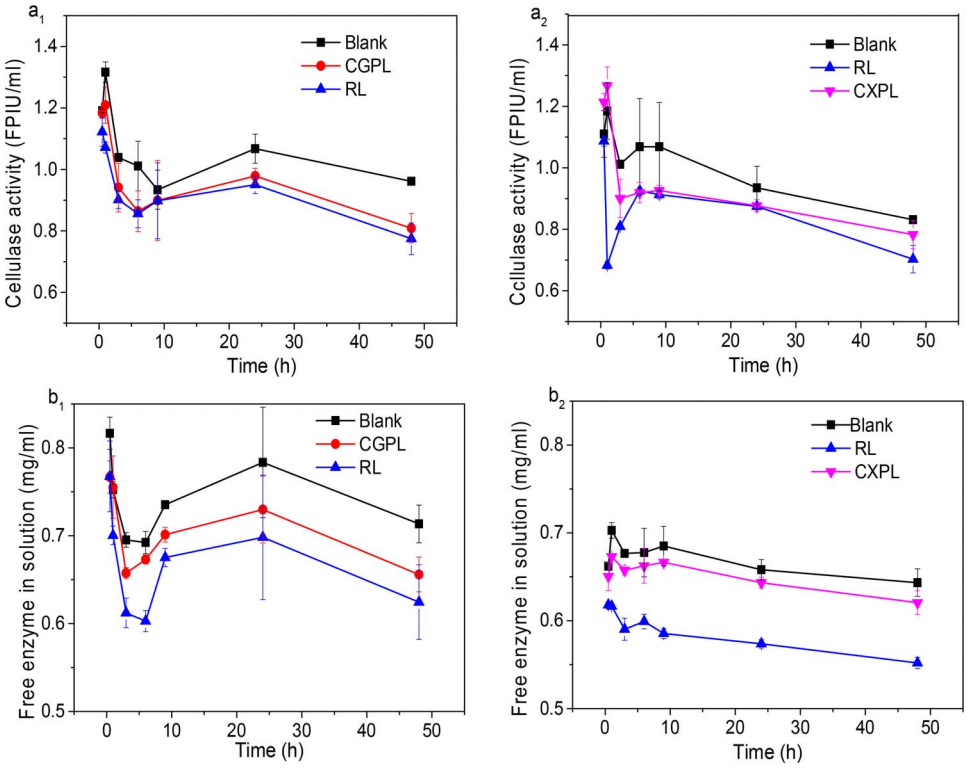

Fig. 5. Influence of CGPL, CXPL, and RL on cellulase properties. a: Filter paper activity of different additions during 48 h at 50 °C. b: Content of free enzymes in the solution with different additions during 48 h at 50 °C.

Table 3
Surface charge and hydrophobic nature of pseudo-lignin and RL.

Samples	Surface charge (mmol/g)	Hydrophobic (ml/g)
RL	−7.00	1665.80
CGPL	−2.67	59.60
CXPL	−4.25	77.45

Table 4
Langmuir adsorption isotherm parameters from enzyme adsorption on samples.

Sample	Γ_{max} (mg/g)	K (ml/mg)	R (L/g)
RL	217.90	13.62	2.97
CGPL	234.71	3.50	0.82
CXPL	277.93	1.31	0.36

structures. Surface charge, hydrophobic nature of pseudo-lignins and cellulase adsorption experiments indicated that pseudo-lignin reduces activity of cellulolytic enzymes through non-productive adsorption. This work provided a more comprehensive display of the inhibitory behaviors of pseudo-lignin formed during biomass pretreatment.

Acknowledgements

The research was supported by the National Natural Science Foundation of China (31570561), the Priority Academic Program Development of Jiangsu Higher Education Institution (PAPD), and Natural Science Foundation of Jiangsu Province for youth (BK20150874) and the Doctorate Fellowship Foundation of Nanjing Forestry University for supporting the work presented in this paper.

References

Baugh, K.D., McCarty, P.L., 1988. Thermochemical pretreatment of lignocellulose to enhance methane fermentation: I. Monosaccharide and furfurals hydrothermal decomposition and product formation rates. Biotechnol. Bioeng. 31, 50–61.

Björkman, A., 1954. Isolation of lignin from finely divided wood with neutral solvents. Nature 174, 1057–1058.

Bradford, M.M., 1976. A rapid and sensitive method for the quantitation of microgram quantities utilizing the principle of protein dye binding. Anal. Biochem. 72, 248–254.

Bulushev, D.A., Ross, J.R., 2011. Catalysis for conversion of biomass to fuels via pyrolysis and gasification: a review. Catal. Today 171, 1–13.

Chang, C., Xiaojian, M.A., Peilin, C.E.N., 2009. Kinetic studies on wheat straw hydrolysis to levulinic acid. Chin. J. Chem. Eng. 17, 835–839.

Chen, W.H., Tu, Y.J., Sheen, H.K., 2010. Impact of dilute acid pretreatment on the structure of bagasse for bioethanol production. Int. J. Energ. Res. 34, 265–274.

Cui, C., Sun, R., Argyropoulos, D.S., 2014. Fractional precipitation of softwood kraft lignin: isolation of narrow fractions common to a variety of lignins. ACS Sustain. Chem. Eng. 2, 959–968.

Donohoe, B.S., Decker, S.R., Tucker, M.P., Himmel, M.E., Vinzant, T.B., 2008. Visualizing lignin coalescence and migration through maize cell walls following thermochemical pretreatment. Biotechnol. Bioeng. 101, 913–925.

Galbe, M., Zacchi, G., 2002. A review of the production of ethanol from softwood. Appl. Microbial. Biotechnol. 59, 618–628.

Ghose, T.K., 1987. Measurement of cellulase activities. Pure. Appl. Chem. 59, 257–268.

Girisuta, B., Janssen, L.P.B.M., Heeres, H.J., 2006. A kinetic study on the decomposition of 5-hydroxymethylfurfural into levulinic acid. Green Chem. 8, 701–709.

Girisuta, B., Janssen, L.P.B.M., Heeres, H.J., 2007. Kinetic study on the acid-catalyzed hydrolysis of cellulose to levulinic acid. Ind. Eng. Chem. Res. 46, 1696–1708.

Hong, J., Ye, X., Zhang, Y.H.P., 2007. Quantitative determination of cellulose accessibility to cellulase based on adsorption of a nonhydrolytic fusion protein containing CBM and GFP with its applications. Langmuir 23, 12535–12540.

Horvat, J., Klaić, B., Metelko, B., Šunjić, V., 1985. Mechanism of levulinic acid formation. Tetrahedron Lett. 26, 2111–2114.

Horvat, J., Klaić, B., Metelko, B., Šunjić, V., 1986. Mechanism of levulinic acid formation in acid catalysed hydrolysis of 2-hydroxymethylfurane and 5-hydroxymethylfurane-2-carhaldehyde. Croat. Chem. Acta 59, 429–438.

Hu, F., Ragauskas, A., 2012. Pretreatment and lignocellulosic chemistry. Bioenerg. Res. 5, 1043–1066.

Hu, F., Jung, S., Ragauskas, A., 2012. Pseudo-lignin formation and its impact on enzymatic hydrolysis. Bioresour. Technol. 117, 7–12.

Hu, F., 2014. Pseudo-Lignin Chemistry in Pretreatment of Biomass for Cellulosic Biofuel Production, Doctoral Dissertation. Georgia Institute of Technology.

Huang, C., He, J., Du, L., Min, D., Yong, Q., 2016a. Structural characterization of the lignins from the green and yellow bamboo of bamboo culm (Phyllostachys pubescens). J. Wood. Chem. Technol. 36, 157–172.

Huang, C., He, J., Min, D., Lai, C., Yong, Q., 2016b. Understanding the nonproductive enzyme adsorption and physicochemical properties of residual lignins in moso bamboo pretreated with sulfuric acid and kraft pulping. Appl. Biochem. Biotechnol. 180, 1508–1523.

Hubbell, C.A., Ragauskas, A.J., 2010. Effect of acid-chlorite delignification on cellulose degree of polymerization. Bioresour. Technol. 101, 7410–7415.

Huber, G.W., Iborra, S., Corma, A., 2006. Synthesis of transportation fuels from biomass: chemistry, catalysts, and engineering. Chem. Rev. 106, 4044–4098.

Jakobsons, J., Hortling, B., Erins, P., Sundquist, J., 1995. Characterization of alkali soluble fraction of steam exploded birch wood. Holzforschung 49, 51–59.
Jung, S., Foston, M., Sullards, M.C., Ragauskas, A.J., 2010. Surface characterization of dilute acid pretreated Populus deltoides by ToF-SIMS. Energy Fuels 24, 1347–1357.
Ko, J.K., Kim, Y., Ximenes, E., Ladisch, M.R., 2015. Effect of liquid hot water pretreatment severity on properties of hardwood lignin and enzymatic hydrolysis of cellulose. Biotechnol. Bioeng. 112, 252–262.
Lai, C., Tu, M., Shi, Z., Zheng, K., Olmos, L.G., Yu, S., 2014. Contrasting effects of hardwood and softwood organosolv lignins on enzymatic hydrolysis of lignocellulose. Bioresour. Technol. 163, 320–327.
Li, J., Henriksson, G., Gellerstedt, G., 2007. Lignin depolymerization/repolymerization and its critical role for delignification of aspen wood by steam explosion. Bioresour. Technol. 98, 3061–3068.
Mosier, N., Wyman, C., Dale, B., Elander, R., Lee, Y.Y., Holtzapple, M., Ladisch, M., 2005. Features of promising technologies for pretreatment of lignocellulosic biomass. Bioresour. Technol. 96, 673–686.
Narron, R.H., Kim, H., Chang, H.M., Jameel, H., Park, S., 2016. Biomass pretreatments capable of enabling lignin valorization in a biorefinery process. Curr. Opin. Biotechnol. 38, 39–46.
Patil, S.K., Lund, C.R., 2011. Formation and growth of humins via aldol addition and condensation during acid-catalyzed conversion of 5-hydroxymethylfurfural. Energy Fuels 25, 4745–4755.
Pielhop, T., Larrazábal, G.O., Studer, M.H., Brethauer, S., Seidel, C.M., von Rohr, P.R., 2015. Lignin repolymerisation in spruce autohydrolysis pretreatment increases cellulase deactivation. Green Chem. 17, 3521–3532.
Pingali, S.V., Urban, V.S., Heller, W.T., McGaughey, J., O'Neill, H., Foston, M., Evans, B.R., 2010. Breakdown of cell wall nanostructure in dilute acid pretreated biomass. Biomacromolecules 11, 2329–2335.
Pu, Y., Hu, F., Huang, F., Davison, B.H., Ragauskas, A.J., 2013. Assessing the molecular structure basis for biomass recalcitrance during dilute acid and hydrothermal pretreatments. Biotechnol. Biofuels 6, 1–13.
Qian, X., Nimlos, M.R., Johnson, D.K., Himmel, M.E., 2005. Acidic sugar degradation pathways. In: Davison, B.H., Evans, B.R., Finkelstein, M., McMillan, J.D. (Eds.), Twenty-Sixth Symposium on Biotechnology for Fuels and Chemicals. Humana Press, Chattanooga, pp. 989–997.
Rasmussen, H., Sørensen, H.R., Meyer, A.S., 2014. Formation of degradation compounds from lignocellulosic biomass in the biorefinery: sugar reaction mechanisms. Carbohydr. Res. 385, 45–57.
Sannigrahi, P., Kim, D.H., Jung, S., Ragauskas, A., 2011. Pseudo-lignin and pretreatment chemistry. Energ. Environ. Sci. 4, 1306–1310.
Sasaki, M., Kabyemela, B., Malaluan, R., Hirose, S., Takeda, N., Adschiri, T., Arai, K., 1998. Cellulose hydrolysis in subcritical and supercritical water. J. Supercrit. Fluids 13, 261–268.
Sluiter, A., Hames, B., Ruiz, R., Scarlata, C., Sluiter, J., Templeton, D., Crocker, D., 2008. Determination of structural carbohydrates and lignin in biomass. Lab. Anal. Proced. 1617, 1–16.
Sun, X., Li, Y., 2004. Colloidal carbon spheres and their core/shell structures with noble-metal nanoparticles. Angew. Chem. Int. Ed. 43, 597–601.
Sun, S., Huang, Y., Sun, R., Tu, M., 2016. The strong association of condensed phenolic moieties in isolated lignins with their inhibition of enzymatic hydrolysis. Green Chem. 18, 4276–4286.
Wen, J.L., Xue, B.L., Xu, F., Sun, R.C., Pinkert, A., 2013. Unmasking the structural features and property of lignin from bamboo. Ind. Crop. Prod. 42, 332–343.
Yang, B., Wyman, C.E., 2006. BSA treatment to enhance enzymatic hydrolysis of cellulose in lignin containing substrates. Biotechnol. Bioeng. 94, 611–617.
Zhuang, J., Wang, X., Xu, J., Wang, Z., Qin, M., 2016. Formation and deposition of pseudo-lignin on liquid-hot-water-treated wood during cooling process. Wood Sci. Technol. 51, 165–174.